

# Interaction between Peroxidase and Cyclooxygenase Activities in Prostaglandin-endoperoxide Synthase

INTERPRETATION OF REACTION KINETICS\*

(Received for publication, July 26, 1993)

Richard J. Kulmacz<sup>‡§</sup>, Robert B. Pendleton<sup>¶||</sup>, and William E. M. Lands<sup>¶\*\*</sup>

From the <sup>‡</sup>Department of Internal Medicine, University of Texas Health Science Center, Houston, Texas 77225 and the <sup>¶</sup>Department of Biochemistry, University of Illinois, Chicago, Illinois 60612

Prostaglandin-endoperoxide synthases have two distinct enzymatic activities in the biosynthesis of prostanooids: a peroxidase and a fatty acid oxygenase. Hydroperoxides, such as the cyclooxygenase reaction product, prostaglandin G<sub>2</sub>, act both as substrates for the synthase peroxidase and as obligatory initiators of the cyclooxygenase reaction itself. A mechanistic scheme was devised to describe the interactions between the two activities of the synthase. This mechanism was based on a heme-dependent peroxidase mechanism such as that observed with horseradish peroxidase and initiation of the cyclooxygenase reaction by intramolecular reaction with a peroxidase intermediate. Rate equations derived from the mechanism were numerically integrated by an interactive computer program that consolidated the diverse phenomena to provide quantitative predictions of the reaction kinetics of the synthase. The predictions agreed well with experimental observations of the purified ovine seminal vesicle enzyme under a wide variety of conditions, including inhibition by exogenous hydroperoxide scavenger and by cyanide, stimulation by exogenous hydroperoxide, and inhibition of eicosapentaenoic acid oxygenation under conditions where arachidonic acid reacts rapidly. The detailed analyses of reaction kinetics made possible with the computer simulation provide important insights into the interactions between the two catalytic activities of the synthase in the control of prostaglandin biosynthesis.

Prostaglandin-endoperoxide synthase catalyzes the two initial reactions in the biosynthesis of prostaglandins, thromboxanes, and prostacyclin (1): a cyclooxygenase reaction that incorporates molecular oxygen into arachidonic acid to form PGG<sub>2</sub><sup>1</sup> and a peroxidase reaction that reduces hydroperoxides

(e.g. PGG<sub>2</sub>) to the corresponding alcohols (e.g. PGH<sub>2</sub>). The reaction kinetics of the synthase are complex and curvilinear, and they include the accelerative actions of peroxidase intermediates in initiating the cyclooxygenase reaction (2) as well as the self-catalyzed inactivation of the cyclooxygenase and the peroxidase activities (3, 4). Thus, analysis of the reaction mechanism of the synthase requires more than conventional steady-state enzyme techniques.

The quantitative relationship between the two catalytic activities has been particularly difficult to understand intuitively. The cyclooxygenase reaction requires the continued presence of hydroperoxides (5, 6), and there is much evidence that the peroxidase plays an important role in the hydroperoxide-dependent initiation of the cyclooxygenase (7). On the other hand, the peroxidase by its very nature decomposes hydroperoxides. This tug of war between hydroperoxide generation and removal in the synthase itself also occurs at the level of the cell, where the balance between hydroperoxide generation and removal may play a deciding role in regulation of prostanooid synthesis (8). That balance has been considered to underlie the different physiological impacts of arachidonate (20:4n-6) and eicosapentaenoate (20:5n-3). It is thus useful to understand in more quantitative biochemical terms the dynamics of the symbiotic interaction between the two catalytic activities in the synthase in interpreting cyclooxygenase-mediated events.

We have developed a mechanism for the synthase based on the heme-dependent peroxidase cycle of horseradish peroxidase; the free radical cyclooxygenase reaction is initiated from an oxidized enzyme intermediate in the peroxidase cycle and propagates in a heme-independent cycle. A computer program was developed to test the validity of the mechanism, to optimize the values of the individual rate constants involved, and to interpret several previously unexplained kinetic phenomena.

The unified mechanistic model accurately predicted the details of the intricate reaction kinetics of prostaglandin biosynthesis under a wide variety of reaction conditions, indicating that the major aspects of the actual reaction mechanism can now be accounted for. The results of the computer simulation of the enzyme reaction provide new insights into the molecular factors controlling cyclooxygenase catalysis. The mechanistic model should be useful in evaluating the roles of putative catalytic intermediates and in analyzing the reaction kinetics of the recently discovered second isoform of the synthase (9, 10).

## MATERIALS AND METHODS

Hematin, TMPD, *N*-ethylmaleimide, GSH, and bovine erythrocyte GSH peroxidase were purchased from Sigma. Arachidonate was from NuChek Preps, Elysian, MN, and EPA was from Cayman Chemical

\* This work was supported in part by Grants GM 30509 and HL 34422 from the United States Public Health Service and by a Pfizer Biomedical Research Award. The costs of publication of this article were defrayed in part by the payment of page charges. This article must therefore be hereby marked "advertisement" in accordance with 18 U.S.C. Section 1734 solely to indicate this fact.

§ To whom correspondence should be addressed: Division of Hematology, Dept. of Internal Medicine, University of Texas Health Sciences Center, P. O. Box 20708, Houston, TX 77225. Tel.: 713-792-5450; Fax: 713-794-4230.

|| Present address: Dept. of Ophthalmology, Northwestern University Medical School, 303 E. Chicago Ave., Chicago, IL 60611.

\*\* Present address: Division of Basic Research, NIAAA, 5600 Fishers La., Rockville, MD 20857.

<sup>1</sup> The abbreviations used are: PGG<sub>2</sub>, prostaglandin G<sub>2</sub>; PGH<sub>2</sub>, prostaglandin H<sub>2</sub>; EPA, 5,8,11,14,17-eicosapentaenoic acid; TMPD, *N,N,N',N'*-tetramethyl-*p*-phenylenediamine; *V*<sub>opt</sub>, maximum cyclooxygenase velocity in a given reaction.

Co., Ann Arbor, MI. PGG<sub>2</sub> and PGG<sub>3</sub> were prepared from arachidonate and EPA, respectively, and purified by thin layer chromatography on silica gel (11).

Prostaglandin-endoperoxide synthase was purified to electrophoretic homogeneity from ovine seminal vesicle microsomes as described (12). The holoenzyme was reconstituted by the addition of hematin (1 mol/mol of subunit). Cyclooxygenase activity was assayed with an oxygen electrode (12). For the standard reaction, the enzyme was injected into 3 ml of 0.1 M potassium phosphate, pH 7.2, containing 1 mM phenol and 100  $\mu$ M arachidonate, thermostatted at 30 °C. Where desired, the electrode signals reflecting oxygen concentration were digitized for storage on magnetic diskettes and subsequent analysis (12). Oxygen and arachidonate remained at essentially saturating levels throughout the reactions. Peroxidase activity was assayed spectrophotometrically with TMPD as cosubstrate (4, 13).

GSH peroxidase activity was assayed essentially as described by Lawrence *et al.* (14). The spectrophotometer cuvette contained 0.1 M potassium phosphate, pH 7.2, 2 mM GSH, 1 mM sodium azide, 0.10 mM NADPH, 0.1 mM EDTA, glutathione reductase (1.25 units/ml), and the GSH peroxidase. The reaction was initiated by the addition of 0.12 mM hydrogen peroxide, and the reaction velocity was calculated from the absorbance decrease at 340 nm using an extinction coefficient of 6.22  $\text{mm}^{-1} \text{cm}^{-1}$ .

For comparison of cyclooxygenase reaction kinetics with arachidonate and EPA, the fatty acids (500  $\mu$ M) in 50 mM Tris, pH 8.5, containing 0.5 mM GSH were treated at room temperature in the dark with GSH peroxidase (200 nmol of GSH/min) for at least 1 h. Then phenol (1 mM) was added, and the solution was kept at room temperature until use. For each reaction, the treated fatty acid solution (300  $\mu$ l) was mixed with 2.7 ml of 0.1 M potassium phosphate, pH 7.2, containing 1 mM phenol in the reaction cuvette thermostatted at 30 °C. About 30 s before the addition of enzyme to start the reaction *N*-ethylmaleimide (75  $\mu$ M) was added to the cuvette to alkylate the remaining GSH.

For evaluation of the sensitivity of the cyclooxygenase activity with EPA to inhibition by GSH peroxidase, the fatty acid was pretreated with a small amount of the peroxidase, as described above, for the kinetic comparison. In this case, however, the cyclooxygenase reaction buffer included 0.55 mM GSH in addition to 1 mM phenol, and no *N*-ethylmaleimide was added. The desired amount of GSH peroxidase was added to the cuvette immediately before injection of the synthase to start the reaction. The amount of GSH peroxidase carried over in the pretreated fatty acid (4 nmol of GSH/min) was negligible compared with the amounts of the peroxidase added directly to the reaction cuvette (25.6–640 nmol of GSH/min).

Computations were performed at various stages on Apple Macintosh SE, Apple Macintosh II, or IBM Model XT machines. The code was written in Microsoft QUICKBASIC language and compiled separately for the particular computer used. Double-precision representation was used for the concentrations of reagents and enzyme intermediates. The Macintosh version of the program (OXYSIM) is available upon request.

The computer program for reaction simulation performs the following series of operations. 1) It reads the default values for the rate constants and the initial reagent concentrations from a disc file. 2) It accepts changes to the values of any of the constants or initial concentrations by keyboard input. The new values can be stored on disc as the default values. 3) It allows systematic variation of a constant or an initial reagent concentration in a series of reaction simulation runs. 4) It allows the length of the simulation run to be specified. To avoid simulations extending past the exhaustion of active enzyme, each run is terminated before the specified time if over 95% of the protein no longer has cyclooxygenase capacity. 5) It logs each simulation run by incorporating the time of that run's start into the disc data file name used for the output. The disc data file also contains the values of the constants and the initial reagent concentrations used. 6) It executes numerical integration of the rate equations using an "initial slope" method with a "flux tolerance" test to set the time increment. This process involves the steps outlined below.

(a) The rate equations that define the mechanism under test are used to calculate the flux through each step in the mechanism with a default time increment of 0.01 s. The rate equations have the conventional form for unimolecular or bimolecular reactions with two exceptions. For cyanide binding, an equilibrium calculation involving the dissociation constant  $K_d$  and the cyanide concentration is used to partition  $E^{\text{III}}$  and  $E^{\text{CN}}$  in the two peroxidase cycles at the start of each interval. This greatly shortens calculation times and can be justified

by the experimentally observed rapid kinetics of cyanide binding (15). Because the cyanide concentration is much greater than the enzyme concentration in the present experiments, the level of free cyanide is assumed to be constant during the reaction. The other exception is for the decomposition of hydroperoxide by added GSH peroxidase. The rate equation used is that described by Flohe and co-workers (16).

(b) The calculated flux into or out of each intermediate is compared with the concentration of that intermediate at the start of the time increment. If the calculated change in the concentration of any intermediate is more than 20% of its initial value, the time increment is decreased by a factor of 10, and all of the fluxes for all of the intermediates are recalculated. If the changes in concentration for all of the intermediates are below the threshold, the calculated fluxes are used to update the concentrations of the intermediates, and the program proceeds to the next time increment. Provision is made for time increments as small as 10 ns.

(c) At the end of each second of simulation, the current concentrations of the key enzyme intermediates and reagents are printed on the screen and on the dot matrix printer and are stored in the disc file. The disc files are in columnar form and can be imported directly into spreadsheet programs for further analysis and graphical presentation.

(d) Before resuming with the next second of simulation, the keyboard is interrogated to check for operator input. If an "S" (for stop) has been typed, execution of the program is halted to allow modification of the concentration of synthase, hydroperoxide, GSH peroxidase, GSH, or peroxidase cosubstrate.

## RESULTS AND DISCUSSION

### Design of Reaction Mechanism

The mechanistic scheme shown in Fig. 1 was designed to reflect known aspects of reaction by the synthase and at the same time keep the number of adjustable parameters to a minimum. The mechanism is built upon the peroxidase cycle elucidated for classic heme-dependent peroxidases such as horseradish peroxidase (17). There is considerable evidence that the synthase peroxidase utilizes such a cycle (4, 18–20). The principal peroxidase cycle is shown as *POX-1* in Fig. 1

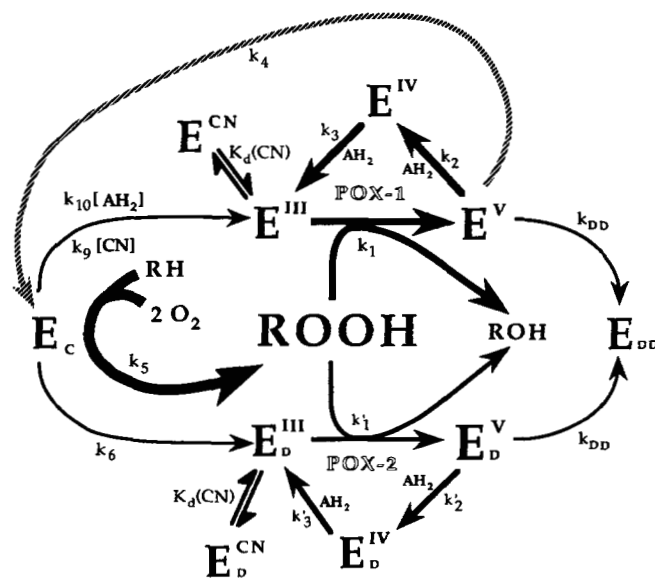


FIG. 1. Mechanistic model for catalysis by the synthase. The roman numerals by the symbol for the enzyme ( $E$ ) indicate the formal oxidation state of the synthase heme iron.  $ROOH$  is hydroperoxide (PGG<sub>2</sub>), and  $ROH$  is the corresponding alcohol (PGH<sub>2</sub>),  $AH_2$  is reducing cosubstrate for the peroxidase,  $E_C$  is the initial cyclooxygenase enzyme intermediate, and  $RH$  is arachidonic acid. Enzyme intermediates in the second peroxidase (*POX-2*) cycle have lost the capacity for cyclooxygenase catalysis, and  $E_{DD}$  is incapable of cyclooxygenase or peroxidase catalysis.

and includes the resting ferric form of the synthase ( $E^{\text{III}}$ ) that reacts with hydroperoxide ( $ROOH$ ), Compound I ( $E^{\text{V}}$ ) that results from this reaction, and Compound II ( $E^{\text{IV}}$ ) that is formed in the first of the two one-electron reductions by cosubstrate ( $AH_2$ ) that lead back to the resting enzyme. To account for self-inactivation of the peroxidase during catalysis (4),  $E^{\text{V}}$  is proposed to decompose in a unimolecular process (rate constant  $k_{DD}$ ) to inactive protein (represented by  $E_{DD}$  in Fig. 1). To account for non-competitive inhibition of the peroxidase by cyanide (21), there is a reversible binding of cyanide, governed by the equilibrium constant  $K_d(\text{CN})$  resulting in catalytically incompetent  $E^{\text{CN}}$ .

Initiation of the cyclooxygenase reaction is proposed to occur by an intramolecular step, governed by rate constant  $k_4$ , that converts  $E^{\text{V}}$  to a catalytic intermediate, represented by  $E_C$ , that may be a tyrosyl radical (7).  $E_C$  interacts as an oxidant with arachidonic acid ( $RH$ ) to abstract a hydrogen atom from C-13 of the fatty acid to give an enzyme-bound fatty acyl radical ( $E_{R\cdot}$ ) that attacks two molecules of molecular oxygen and rearranges to form the enzyme-bound PGG<sub>2</sub> radical ( $E_{ROO\cdot}$ ). To complete the cyclooxygenase cycle, a hydrogen atom is transferred from the enzyme to produce PGG<sub>2</sub> and to regenerate  $E_C$ , and the PGG<sub>2</sub> dissociates from the enzyme.  $E_{R\cdot}$  and  $E_{ROO\cdot}$  are not explicit in the mechanism shown in Fig. 1. Instead, the rate of the oxygenation reaction is described with the rate constant  $k_5$ , which refers to the rate-determining step in the interconversions of the cyclooxygenase cycle intermediates. This simplification was made because the aggregate rate of the cyclooxygenase cycle can be estimated from the specific activity, whereas the individual rate constants are as yet inaccessible.

To account for inhibition of the cyclooxygenase at high levels of peroxidase cosubstrate (6), the cosubstrate is postulated to act also as a reductant to quench  $E_C$  back to resting enzyme in a process governed by rate constant  $k_{10}$ . Precedents for such a process include the quenching of tyrosyl radical in the synthase by peroxidase cosubstrates (22) and two-electron oxidation of acetaminophen during cyclooxygenase catalysis (23).

In the presence of phenol, moderate levels of cyanide (5–30 mM) have been found to slow the acceleration and decrease the velocity of the cyclooxygenase (6, 21). These concentrations of cyanide are considerably higher than those needed to saturate the synthase heme ( $K_d = 0.2$  mM) (21), suggesting a second mechanism of interaction between cyanide and the synthase, an action at the cyclooxygenase itself. Because cyanide has been shown to be able to act as reductant (24), quenching of  $E_C$  by cyanide was incorporated into the reaction mechanism (rate constant  $k_9$ ; Fig. 1).

Cyclooxygenase self-inactivation is proposed to result from an intramolecular collapse of  $E_C$  regulated by constant  $k_6$ , to form  $E_D$ . To account for the observation that the majority of the peroxidase activity remains after self-inactivation of the cyclooxygenase (13),  $E_D$  is proposed to lack cyclooxygenase activity although it still participates in peroxidase catalysis (shown as the  $POX-2$  cycle) until inactivation via  $k_{DD}$  to  $E_{DD}$ .

Included in the computer model, but not shown in Fig. 1, is the participation by GSH peroxidase, added in some experiments as a hydroperoxide scavenger. The mechanism of this enzyme and its rate equations in reducing hydroperoxides to alcohols at the expense of GSH are well known (16). GSH peroxidase is assumed not to interact directly with the synthase but to exert its effect solely in removing hydroperoxide activators.

### Estimation of Rate Constants

The values of the various rate constants indicated in Fig. 1 used for the computer simulations are presented in Table I. The values of some of the constants have been determined experimentally, although usually at temperatures below 30 °C, the temperature used for most of the experimental cyclooxygenase assays. The measured cyclooxygenase rate approximately doubles with a 10 °C increase in temperature, as do the few peroxidase reaction steps examined.<sup>2</sup> Thus, as a first approximation, rate constants were assumed to increase by a factor of 2 for each 10 °C increase in temperature. A similar adjustment was used with GSH peroxidase, which was assayed at 23 °C but used in cyclooxygenase reactions at 30 °C. References for experimentally determined values are also presented in Table I. A more detailed description of the rationale for the values assigned to individual rate constants is presented below.

Several experimental estimates of the value of  $k_1$  have been determined for various hydroperoxides and reaction conditions. The value used in the computer simulation,  $7 \times 10^7 \text{ M}^{-1} \text{ s}^{-1}$ , is that determined for PGG<sub>2</sub> (20) multiplied by a factor of 2 to account for the 10 °C higher temperature used here. Comparable values were obtained in the present study for PGG<sub>2</sub> and PGG<sub>3</sub> (see below and Table I).

The value of  $k_3$  for phenol,  $1.5 \times 10^6 \text{ M}^{-1} \text{ s}^{-1}$ , was estimated from earlier values with TMPD as the cosubstrate (4). The recent value reported by Hsuanyu and Dunford (25) is in reasonable agreement. Reported values of  $k_2$  are considerably higher than the corresponding values for  $k_3$  for the same cosubstrate (26), establishing  $k_3$  as the rate-limiting step in the peroxidase reaction under most conditions. To reflect this, the value of  $k_2$  was set at 10 times that of  $k_3$ . The oxidized peroxidase intermediates are known to return spontaneously to the resting ferric state in the absence of added cosubstrate (18–20), presumably due to endogenous reductants present in the protein preparation. However, the rates of these reactions are relatively slow compared with those dependent on added cosubstrate and have not been considered in the present treatment.

The values of  $k'_1$ ,  $k'_2$ , and  $k'_3$  in the second peroxidase cycle (shown as  $POX-2$  in Fig. 1) were fixed at 70% of the corresponding values in the first peroxidase cycle ( $POX-1$ ) to reflect the partial inactivation of the peroxidase that accompanies self-inactivation of the cyclooxygenase (13). The self-inactivating event was assumed to be the same for both peroxidase cycles, and so the same value for the pertinent rate constant,  $k_{DD}$ , was used for both. This approach avoids introducing additional adjustable parameters for the second peroxidase cycle.

An unambiguous experimental estimate for the rate of the intramolecular conversion of  $E^{\text{V}}$  to  $E_C$  ( $k_4$ ) is not available. The rate of the conversion of  $E^{\text{V}}$  to the next spectrally distinct species in the absence of added cosubstrates was estimated to be  $65 \text{ s}^{-1}$  (20). These authors concluded that the second optical intermediate represented the cyclooxygenase oxidant (a tyrosine radical in their hypothesis). However, significant amounts of endogenous reductant appear to be present even in rigorously purified enzyme, as evidence by the spontaneous return of oxidized intermediates to the resting ferric state in the absence of added cosubstrate (18–20). This makes it quite possible that the second optical intermediate observed by Dietz *et al.* (20) was actually the second peroxidase intermediate,  $E^{\text{IV}}$ . Simulation of the overall reaction with a wide range of values for  $k_4$  indicated that a realistic acceleration of

<sup>2</sup> R. J. Kulmacz and A.-L. Tsai, unpublished results.

TABLE I  
 Values of constants used for computer simulation of reaction at 30 °C

Constant (see Fig. 1)	Value	Literature value
$k_1$	$7 \times 10^7 \text{ M}^{-1} \text{ s}^{-1}$	$3.5 \times 10^7 \text{ M}^{-1} \text{ s}^{-1}$ (PGG <sub>2</sub> ; 20 °C) <sup>a</sup> $2.1 \times 10^7 \text{ M}^{-1} \text{ s}^{-1}$ (PGG <sub>2</sub> ; 25 °C) <sup>b</sup> $1.3 \times 10^7 \text{ M}^{-1} \text{ s}^{-1}$ (PGG <sub>3</sub> ; 25 °C) <sup>b</sup>
$k_2$	$1.5 \times 10^7 \text{ M}^{-1} \text{ s}^{-1}$	
$k_3$	$1.5 \times 10^6 \text{ M}^{-1} \text{ s}^{-1}$	$5.3 \times 10^6 \text{ M}^{-1} \text{ s}^{-1}$ (4 °C) <sup>c</sup>
$k_4$	$1.75 \times 10^3 \text{ s}^{-1}$	
$k_5$	$90 \text{ s}^{-1}$	
$k_6$	$0.07 \text{ s}^{-1}$	$0.1 \text{ s}^{-1}$ (23 °C) <sup>d</sup>
$k_{DD}$	$0.38 \text{ s}^{-1}$	$0.22 \text{ s}^{-1}$ (23 °C) <sup>e</sup>
$k_9$	$22 \text{ M}^{-1} \text{ s}^{-1}$	
$k_{10}$	$1750 \text{ M}^{-1} \text{ s}^{-1}$	
$K_d$ (CN)	$0.2 \text{ mM}$	$0.19 \text{ mM}$ <sup>f</sup> $0.065 \text{ mM}$ (pH 8.0, 4 °C) <sup>g</sup>
Autoxidation	$1 \times 10^{-9} \text{ M s}^{-1}$	
ROOH <sub>init</sub>	$2 \times 10^{-9} \text{ M}$	
GSH peroxidase (GSP) kinetics $v$ (GSP) = $\frac{[\text{GSP}]}{P_1 + [\text{ROOH}] + P_2 + [\text{GSH}]}$		
$P_1$ (GSP)	$5 \times 10^{-8} \text{ M s}$	$3\text{--}13 \times 10^{-8} \text{ M s}$ <sup>h</sup>
$P_2$ (GSP)	$2.2 \times 10^{-6} \text{ M s}$	$2.2 \times 10^{-6} \text{ M s}$ <sup>h</sup>

<sup>a</sup> Ref. 20.<sup>b</sup> Present study.<sup>c</sup> Ref. 25.<sup>d</sup> Ref. 6.<sup>e</sup> Ref. 28.<sup>f</sup> Ref. 21.<sup>g</sup> Ref. 15.<sup>h</sup> Ref. 16.

the cyclooxygenase was predicted when the value of  $k_4$  was set to  $1750 \text{ s}^{-1}$ . Lower values resulted in unrealistically slow acceleration, and higher values resulted in overly rapid acceleration.

The value of  $k_5$  is based on the observed cyclooxygenase specific activity for purified ovine synthase. A typical specific activity of 100 nmol of O<sub>2</sub>/min/μg of protein translates to 58 mol of arachidonate/s/mol of synthase subunit. Assuming that two-thirds of the synthase is present as  $E_C$  at the time the maximal cyclooxygenase velocity ( $V_{\text{opt}}$ ) is reached gives an estimated value for  $k_5$  of  $90 \text{ s}^{-1}$ .

Cyclooxygenase activity decays at a roughly exponential rate during reaction with arachidonate (3, 6); the slope of a semilog plot of the velocity as a function of time can be used to obtain an estimate for the rate constant ( $k_6$ ) of self-inactivation of the cyclooxygenase during conversion of fatty acid to prostaglandin. The value used in the present simulations,  $0.07 \text{ s}^{-1}$ , is somewhat lower than previous estimates (6) because the entire curve was considered here rather than just the steep initial decline in velocity. A similar estimate for  $k_6$  can be obtained by dividing the maximal cyclooxygenase velocity by the ultimate extent of oxygen consumption in a given reaction (3).

Inactivation of both cyclooxygenase and peroxidase activities by conversion of  $E^V$  to  $E_{DD}$  via  $k_{DD}$  (in both peroxidase cycles of Fig. 1) was postulated to account for the observed loss of the activities during exposure of the synthase to hydroperoxides in the absence of cyclooxygenase substrates (4, 27, 28). In reactions involving fatty acid hydroperoxide, the rate equation was found (28) to have both hydroperoxide-dependent (rate constant =  $1.9 \times 10^4 \text{ M}^{-1} \text{ s}^{-1}$  at 23 °C) and hydroperoxide-independent (rate constant =  $0.22 \text{ s}^{-1}$  at 23 °C) terms. For most of the reactions with arachidonate examined here, the hydroperoxide levels peak in the micromolar range, and, therefore, the hydroperoxide-independent term predominates. Accordingly, only the hydroperoxide-independent term was included in the present simulations. The value used for

$k_{DD}$ ,  $0.38 \text{ s}^{-1}$ , reflects an adjustment for temperature.

The value of  $k_9$ , which governs the reduction of  $E_C$  to resting enzyme by cyanide (Fig. 1), was adjusted so as to fit the extended lag times seen with 5–30 mM levels of this agent in the presence of phenol (21). A value of  $22 \text{ M}^{-1} \text{ s}^{-1}$  gave a reasonable fit to the experimental data.

The value of  $k_{10}$ , which governs the reduction of  $E_C$  to resting enzyme by peroxidase cosubstrate (Fig. 1), was set empirically at  $1750 \text{ M}^{-1} \text{ s}^{-1}$  to obtain a reasonable prediction of the sensitivity of the cyclooxygenase to inhibition by GSH peroxidase (see below). It should be noted that although  $k_4$  and  $k_{10}$  are numerically equivalent and  $k_{10}$  seems much larger than  $k_5$ ,  $k_4$  and  $k_5$  are unimolecular rate constants, whereas  $k_{10}$  is a bimolecular rate constant. Thus, at 1 mM phenol, the rate of quenching of  $E_C$  is initially much smaller than its rate of formation or the rate of arachidonate oxygenation.

The value used for the dissociation constant of the cyanide-synthase complex,  $K_d(\text{CN})$ , was 0.2 mM, essentially identical to that determined spectrophotometrically (21). A 3-fold lower value (65 μM) has been reported from measurements made at a higher pH and lower temperature (15).

A hydroperoxide level of 2 nM (0.002% of the initial arachidonate) was used to approximate initial conditions, and the rate of non-enzymatic fatty acid oxidation was fixed at  $1 \text{ nM s}^{-1}$  to simulate autoxidation of arachidonate in the aqueous reaction system.

Values for the kinetic constants of GSH peroxidase were taken from the literature (16).

#### Validation of Numerical Integration Routine

Several procedures were used to ensure that the computer program was performing the numerical integration in a satisfactory manner.

(a) The output concentrations for enzyme, substrate, and products were routinely examined to ensure the absence of abrupt changes or unreasonably large or small values. Setting a flux tolerance limit value of 0.2 in the program resulted in

a smooth progression of oxygen consumption. Although smaller values for the limit did result in smoother concentration *versus* time curves for some reaction intermediates, computation time was greatly increased without significant changes in the predicted reaction course (29).

(b) The number of computational cycles executed was examined to ensure that the time increment used was appropriate to the values of the rate constants and the intermediate concentrations. In general, very small time increments were needed only where the concentrations of enzyme intermediates were rising from an initial value of 0 in the first s or so of a simulated reaction or for reactions in which the initial hydroperoxide concentration was much above 10  $\mu\text{M}$ .

(c) Simulated reactions were run successfully with the same set of parameter values on different computers. The results with the IBM computer, the Macintosh SE, and the Macintosh II were almost identical (less than 1% difference in predicted intermediate concentration at a given time), ruling out a machine-specific artifact.

#### Validation of Proposed Reaction Mechanism

The validity of the reaction mechanism used in the computer model was evaluated by comparison of the predicted reaction characteristics with the results obtained experimentally under a wide variety of conditions with the pure ovine synthase. These conditions are presented individually below. With the values of rate constants shown in Table I, the computer model predicted a cyclooxygenase specific activity of 100  $\mu\text{mol}$  of  $\text{O}_2/\text{min}/\text{mg}$  of protein under standard conditions, a value that is about average for our preparations of homogeneous sheep seminal vesicle enzyme. To compensate for differences in specific activity between batches of the synthase, the concentration of synthase in the computer model was adjusted to give a cyclooxygenase activity equal to the control activity in the particular experiment used for comparison.

**Inhibition of Cyclooxygenase by GSH Peroxidase**—The addition of hydroperoxide scavenger, GSH peroxidase, decreases both the velocity and the ultimate extent of the cyclooxygenase reaction (30). Accordingly, the computer model was used to predict the catalytic behavior of the cyclooxygenase in the presence of several different levels of GSH peroxidase activity up to 40  $\mu\text{M}$  peroxide/s. The predictions are compared with experimental results from pure synthase and similar levels of hydroperoxide scavenger enzyme in Fig. 2. The predicted cyclooxygenase velocity and extent declined linearly as the level of added GSH peroxidase was increased, just as observed experimentally. The GSH peroxidase activity predicted to be needed for complete suppression of the cyclooxygenase was essentially the same as the experimental value.

Analysis of the concentrations of intermediates during simulated reactions with and without GSH peroxidase provided a detailed explanation for the coordinate decreases in cyclooxygenase velocity and the ultimate extent of reaction. Exogenous peroxidase lowers the hydroperoxide level during all phases of the simulated reaction with the result that the rate of  $E_C$  formation (via the  $k_1$  and  $k_4$  steps) is decreased relative to the rate of  $E_C$  depletion (via the irreversible  $k_6$  step and the  $k_{10}$  step). The peak level of  $E_C$  is thus decreased, and with it, the cyclooxygenase  $V_{\text{opt}}$  is decreased. Because the rate of quenching via  $k_{10}$  is faster than that of self-inactivation via  $k_6$  (with millimolar phenol), as the rate of  $E_C$  formation drops, enzyme accumulates as  $E^{\text{III}}$  (latent enzyme) rather than as  $E_D$ . The cyclooxygenase activity thus comes to a stop with some enzyme still not self-inactivated.

In earlier experiments (30), the presence of latent cycloo-

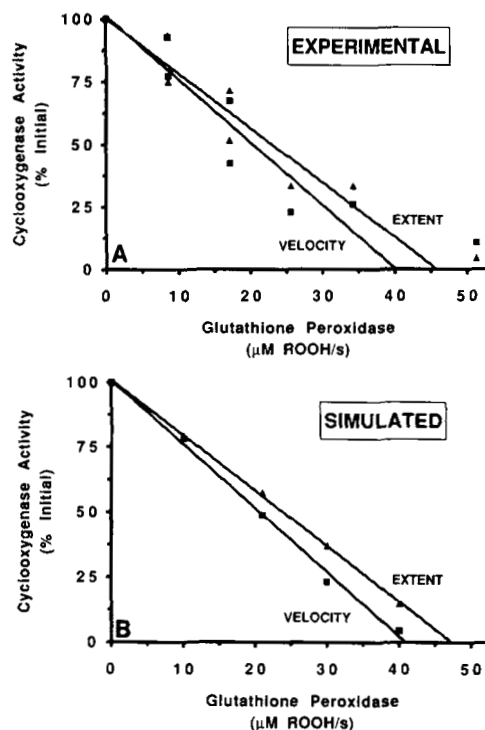


FIG. 2. Inhibition of cyclooxygenase velocity and reaction extent by GSH peroxidase. The reactions at 30 °C contained 0.67 mM phenol, 0.5 mM GSH, and the indicated levels of GSH peroxidase (assayed at 23 °C). Panel A shows experimental results taken from Ref. 21. Panel B shows predictions from the computer model. The maximum cyclooxygenase velocities ( $V_{\text{opt}}$ ) are represented by squares, and the eventual limits of oxygen consumption (extent) are indicated by triangles.

xygenase in the later stages of a GSH-suppressed reaction was demonstrated by observation of a burst of cyclooxygenase activity after addition of *N*-ethylmaleimide to alkylate GSH and stop GSH peroxidase activity. This response is seen with the simulated reaction in Fig. 3A. For this, the simulation was interrupted after 50 s to decrease the GSH concentration to 0 (as if *N*-ethylmaleimide was added) and then resumed. A second burst of cyclooxygenase activity occurred with a  $V_{\text{opt}}$  and extent corresponding to the difference between the values in the control and those in the presence of GSH peroxidase before intervention to remove GSH.

Addition of GSH peroxidase after initiation of cyclooxygenase was found to suppress further cyclooxygenase activity (6) indicating that a continued presence of hydroperoxide is required to maintain cyclooxygenase activity. The computer simulation predicts just such behavior (Fig. 3B). In this regard, the quenching process governed by  $k_{10}$  is central to the prediction of a continuous requirement for hydroperoxide activator; without such quenching, initiation of enough cyclooxygenase to get an initial burst of activity eventually results in initiation of all of it, leaving no latent enzyme.

**Inhibition of Cyclooxygenase Velocity and Acceleration by Cyanide**—In the presence of phenol, increasing the concentration of the heme ligand, cyanide, decreases  $V_{\text{opt}}$  and the acceleration of the cyclooxygenase (evident from the longer time needed to reach  $V_{\text{opt}}$ ) without appreciably changing the ultimate extent of cyclooxygenase reaction (21) (Fig. 4). The reaction kinetics predicted from the mechanistic model (Fig. 4) agree reasonably well with the experimental data, indicating that the action of cyanide to inhibit the peroxidase activity is sufficient to account for the ligand's effects on the cyclooxygenase activity under these conditions.

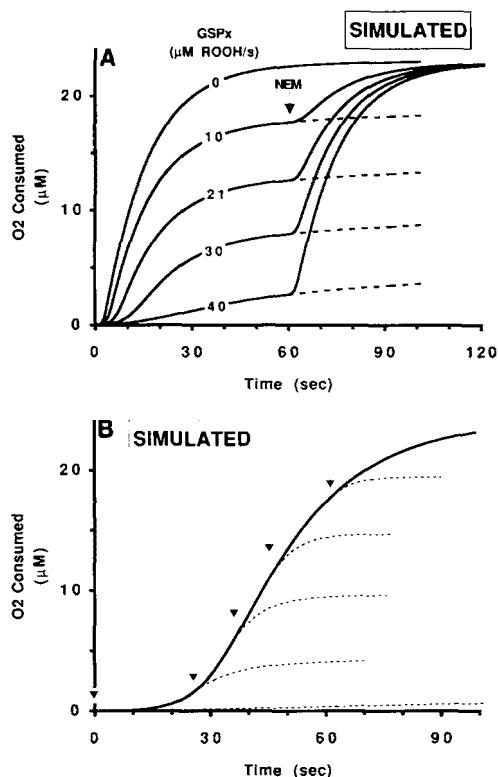


FIG. 3. Predicted effects of delayed addition or removal of GSH peroxidase (GSPx) activity. Panel A, the GSH level was decreased to 0 at the indicated time after initiation of a simulated reaction of 11.6 nM synthase in the presence of the indicated levels of GSH peroxidase (in micromolar ROOH/s) under the conditions described in the legend to Fig. 2. The dashed line indicates the simulated reaction trajectory when the GSH level was not changed. Panel B, the GSH peroxidase level was increased to 2.0  $\mu\text{M}$  ROOH/s at the indicated times after initiation of the simulated reaction of 11.6 nM synthase in the presence of 5 mM cyanide and 1 mM phenol. The values of rate constants are those shown in Table I. NEM, N-ethylmaleimide.

Addition of exogenous hydroperoxide to a cyclooxygenase reaction inhibited by phenol and cyanide causes faster acceleration of the cyclooxygenase reaction and decreases the time needed to reach  $V_{\text{opt}}$  (lag time) (31). This aspect of kinetic behavior forms the basis for a quantitative assay for hydroperoxides (32). The computer model correctly predicts the decrease in lag time upon the addition of hydroperoxides in reactions containing several different levels of cyanide (Fig. 5).

Suppression of the cyclooxygenase  $V_{\text{opt}}$  occurs at lower levels of GSH peroxidase with cyanide present (21), and the computer model predicts the observed behavior quite accurately (Fig. 6).

#### Stimulation of Cyclooxygenase by Phenol

Peroxidase cosubstrates such as phenol are known to increase, in parallel, both the cyclooxygenase  $V_{\text{opt}}$  and the ultimate event of cyclooxygenase catalysis before self-inactivation (21). In simulated reactions, the conventional actions of peroxidase cosubstrates in reducing  $E^{\text{V}}$  to  $E^{\text{IV}}$  and to  $E^{\text{III}}$  (Fig. 1) were able to stimulate the cyclooxygenase velocity somewhat, but they had no significant effect on the extent of cyclooxygenase catalysis before self-inactivation (data not shown). Based on the ability of tryptophan to stimulate the cyclooxygenase without being appreciably oxidized (33), an alternative, catalytic action of the cosubstrates is proposed. This action is viewed as a facilitation by bound cosubstrate

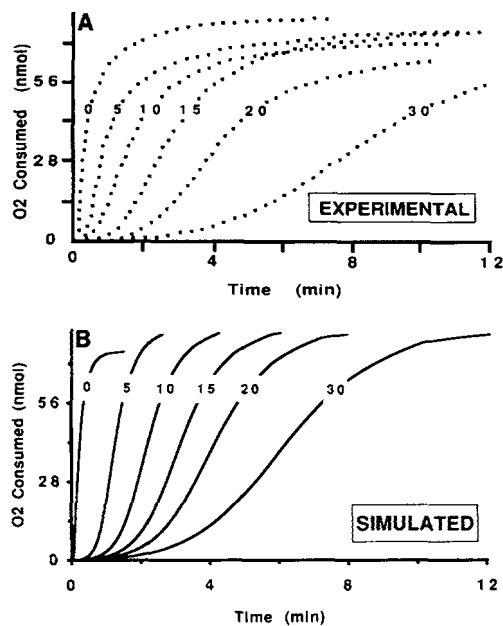


FIG. 4. Inhibition of cyclooxygenase velocity and acceleration by cyanide. The reactions contained 1.0 mM phenol and the indicated concentrations of sodium cyanide. Panel A shows experimental results taken from Ref. 21. Panel B shows predictions from the computer model.

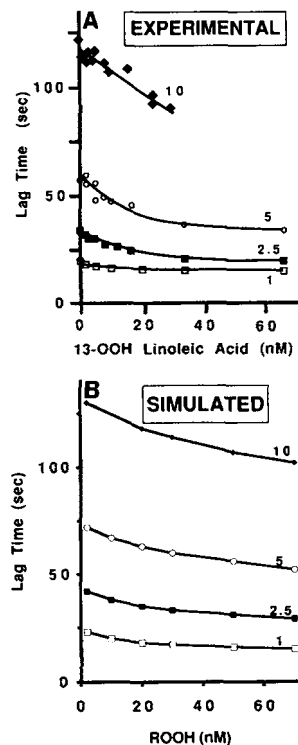


FIG. 5. Reduction of lag time in cyanide-inhibited cyclooxygenase by added lipid hydroperoxide. The reactions contained 1.0 mM phenol and the indicated levels of sodium cyanide (millimolar) and hydroperoxide. Panel A shows experimental results taken from Ref. 31. Panel B shows predictions from the computer model.

of electron transfer in one of the steps in the cyclooxygenase catalytic cycle. This facilitation is envisioned to involve a reversible oxidation of the cosubstrate and thereby increase the rate of cyclooxygenase catalysis (via  $k_5$ ) relative to that of the self-inactivation process (via  $k_6$ ).

To simulate this direct effect of cosubstrates on the cycloo-

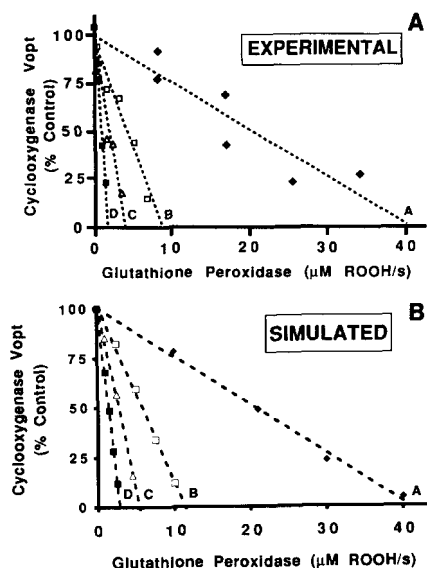


FIG. 6. Increased sensitivity of cyanide-inhibited cyclooxygenase to inhibition by GSH peroxidase. The reactions contained 0.67 mM phenol, 0.5 mM GSH, and the indicated levels of sodium cyanide and GSH peroxidase. Panel A shows experimental results taken from Ref. 21, with cyanide concentration of 0 (A), 0.5 (B), 1.25 (C), or 2.5 mM (D). Panel B shows predictions from the computer model.

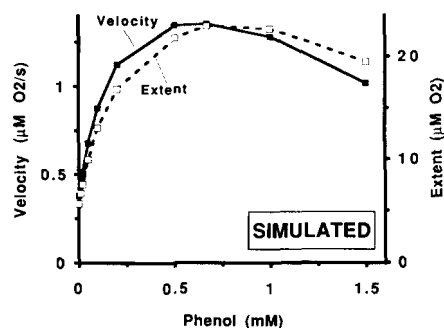


FIG. 7. Predicted effects of phenol on cyclooxygenase velocity and ultimate reaction extent. Predictions of velocity (solid symbols) and extent (open symbols) were from computer simulation using the rate constants shown in Table I and an enzyme concentration of 11.6 nM.

ygenase in the computer model,  $k_5$  is modified by the factor, for  $(0.2 + 0.8/(1 + K_m(AH_2)/[AH_2]))$ . The 0.2 term reflects the portion of cyclooxygenase velocity observed without added cosubstrate; the second term reflects the saturable binding of the cosubstrate governed by the constant  $K_m(AH_2)$ . The value of  $K_m(AH_2)$  for phenol was estimated to be 0.2 mM (21). Simulated reactions of the synthase with arachidonate at several levels of phenol between 0 and 1 mM (Fig. 7) show that the model now predicts successfully that both the cyclooxygenase velocity and its ultimate extent are increased by cosubstrate in a fashion similar to that observed experimentally (21).

#### Cyclooxygenase Kinetics with Eicosapentaenoic Acid

Conversion of eicosapentaenoic acid (EPA) to prostaglandin has been considered to require considerably more hydroperoxide than does conversion of arachidonate (34). The specific activity of the cyclooxygenase and the number of catalytic turnovers before cessation of activity with EPA were about 10% of those observed with arachidonate (Fig. 8A). Two possible explanations were evaluated: (a) PGG<sub>3</sub> produced

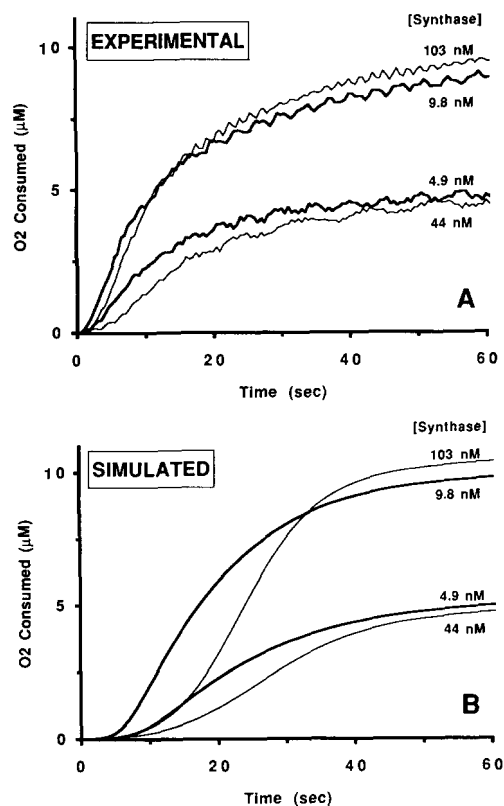


FIG. 8. Comparison of cyclooxygenase reaction kinetics with arachidonate and EPA. Panel A shows experimental data obtained with 50  $\mu$ M arachidonate (boldface lines) or EPA (lightface lines) and the indicated concentrations of synthase subunit, as described under "Materials and Methods." The specific activity of the synthase used was 48  $\mu$ mol of O<sub>2</sub>/min/mg of protein. Panel B shows reaction kinetics predicted using the parameters given in Table I, with  $k_5$  set at 90  $M^{-1} s^{-1}$  for arachidonate (boldface lines) or 23.5  $M^{-1} s^{-1}$  for EPA (lightface lines), with the indicated amounts of synthase and the specific activity used in panel A, as described in the text.

from EPA is a poorer substrate for the peroxidase (i.e. the rate constant  $k_1$  is smaller than that for PGG<sub>2</sub>) resulting in less efficient initiation of the cyclooxygenase, or (b) EPA is a poorer substrate for the cyclooxygenase (i.e. the rate of  $k_5$  is smaller than that for arachidonate).

A direct analysis of the synthase peroxidase kinetics with PGG<sub>2</sub> and PGG<sub>3</sub> as substrate was carried out using procedures described for 15-hydroperoxyeicosatetraenoic acid (4). The experimentally determined value of  $k_1$  for PGG<sub>2</sub> was  $2.1 \pm 0.7 \times 10^7 M^{-1} s^{-1}$ ; for PGG<sub>3</sub> it was  $1.3 \pm 0.4 \times 10^7 M^{-1} s^{-1}$ . The value for PGG<sub>3</sub> is not significantly different from that for PGG<sub>2</sub>, indicating that the two hydroperoxides were comparably effective as substrates for the synthase peroxidase. Thus, it is likely that the altered reaction kinetics with EPA are caused by differences in the rate of propagation of the cyclooxygenase reaction rather than in the rate of its initiation.

Accordingly, the computer model was used to examine the effect of two different values of  $k_5$ : 90  $M^{-1} s^{-1}$  (for arachidonate) and 23.5  $M^{-1} s^{-1}$  (for EPA). Two different enzyme levels were examined with each setting of  $k_5$  to mimic the two experimental enzyme levels (Fig. 8A). It can be seen that with only this decrease in  $k_5$ , the model predicted decreases in both cyclooxygenase  $V_{opt}$  and reaction extent (Fig. 8B), comparable with those observed experimentally (Fig. 8A).

The adequacy of a decrease in the value of  $k_5$  to account for the kinetics of the reaction with EPA was further tested by examining the predicted inhibitory effect of GSH peroxidase on the cyclooxygenase, just as was done with arachidon-

ate in Fig. 2. Experimental data for suppression of the cyclooxygenase  $V_{opt}$  by GSH peroxidase in reactions with EPA are shown in Fig. 9, along with the two sets of predictions from the computer model (using  $k_5 = 23.5$  or  $90 \text{ M}^{-1} \text{ s}^{-1}$ ). Experimentally, 50% inhibition was seen at a GSH peroxidase/cyclooxygenase ratio of about 7 with EPA and about 30 with arachidonate. This agrees with earlier observations of stronger inhibition of the cyclooxygenase with EPA (34). The simulations predicted (Fig. 9) that the lower value of  $k_5$  leads to an increased sensitivity to inhibition by GSH peroxidase, with 50% inhibition at a GSH peroxidase/cyclooxygenase ratio of about 9; the corresponding prediction for arachidonate was a ratio of about 30. These predicted values agree reasonably well with the experimental ones. Thus, the dramatically impaired cyclooxygenase kinetics with EPA can be explained to a first approximation by a slower rate of propagation of the cyclooxygenase reaction with the *n*-3 fatty acid than with the *n*-6 fatty acid. The acceleration in simulated reactions with EPA was somewhat slower than that experimentally observed, as evidenced by the longer time needed to achieve  $V_{opt}$  (Fig. 8). This minor discrepancy suggests that the change in substrate may have secondary effects on other steps besides  $k_5$ , as proposed earlier (35).

Analysis of the concentrations of individual enzyme intermediates during the simulations of reaction with EPA shown in Fig. 8B revealed that less than half of the synthase had self-inactivated at the point where cyclooxygenase activity had almost stopped. Thus, the simulation predicted that complete self-inactivation was not the cause of cessation of cyclooxygenase catalysis in reactions with EPA. Because the cyclooxygenase reaction was also found to stop before complete self-inactivation when the system was suppressed with GSH peroxidase (Fig. 2), it was suspected that insufficient hydroperoxide levels might account for the behavior with EPA as well. To test this possibility, a two-part simulation of the reaction with EPA was performed in which  $1 \mu\text{M}$  hydroperoxide was "added" to the computation at 65 s. The model predicted a second burst of cyclooxygenase activity (Fig. 10), confirming that the hydroperoxide level was indeed limiting the cyclooxygenase velocity.

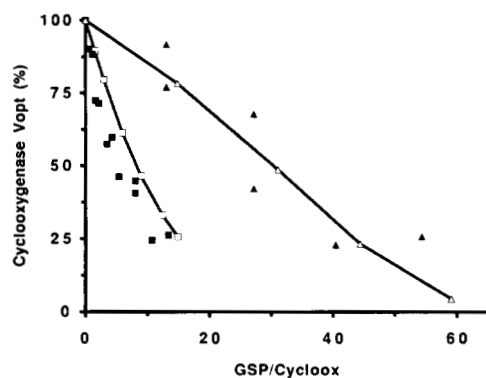


FIG. 9. Inhibition of cyclooxygenase (*Cycloo*) velocity by GSH peroxidase (*GSP*) with EPA or arachidonate as substrate. For reactions with EPA, the experimental data are represented by *solid squares*, and the model predictions are represented by *open squares*. Details are described under "Materials and Methods." For reactions with arachidonate, experimental data (*solid triangles*) and model predictions (*open triangles*) are taken from Fig. 2. The amounts of added GSH peroxidase (in nanomoles of hydroperoxide reduced per min, assayed at  $23^\circ\text{C}$ ) have been normalized to the initial cyclooxygenase activity (in nanomoles of  $\text{PGG}_2$  produced per min, assayed at  $30^\circ\text{C}$ ) to account for the different control activities in the experiments with EPA ( $24 \text{ nmol of } \text{PGG}_2/\text{min}$ ) and arachidonate ( $113 \text{ nmol of } \text{PGG}_2/\text{min}$ ).

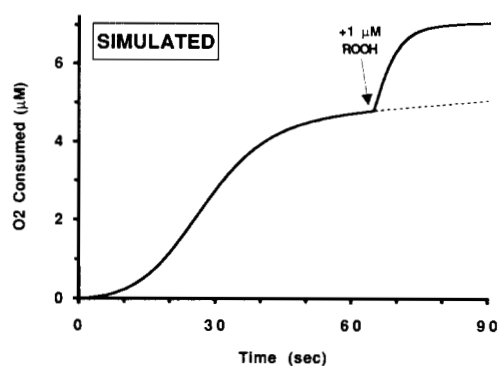


FIG. 10. Prediction of latent cyclooxygenase activity during reaction with EPA. Computer simulation of the reaction of  $44 \text{ nM}$  synthase with EPA was performed as described in the legend to Fig. 8. The simulation was interrupted at 65 s, and the hydroperoxide level was either increased by  $1 \mu\text{M}$  (*solid line*) or left unchanged (*dashed line*).

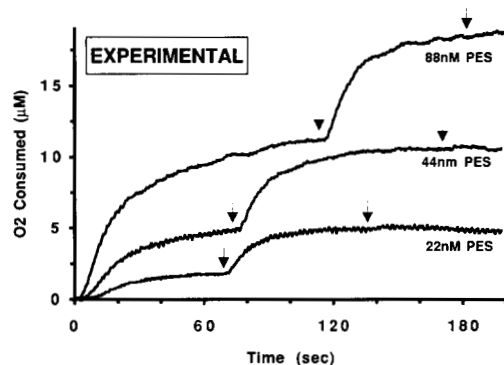


FIG. 11. Demonstration of latent cyclooxygenase activity during reaction with EPA. The indicated concentrations of the synthase were reacted with  $50 \mu\text{M}$  EPA in  $0.1 \text{ M}$  potassium phosphate, pH 7.2, containing  $1 \text{ mM}$  phenol and  $50 \mu\text{M}$  GSH at  $30^\circ\text{C}$ . Hydrogen peroxide ( $150 \mu\text{M}$ ) was added at the points indicated by the *arrows*. *PES*, prostaglandin-endoperoxide synthase.

This prediction of latent cyclooxygenase activity upon cessation of cyclooxygenase activity in reactions with EPA was unexpected, and so it was tested experimentally (Fig. 11). Reactions of EPA with three different levels of the synthase were allowed to proceed until oxygen consumption had almost stopped, and then  $150 \mu\text{M}$  hydrogen peroxide was injected. This hydrogen peroxide concentration is roughly equivalent to  $200 \text{ nM}$  lipid hydroperoxide in terms of the ability to initiate the cyclooxygenase (36). In each case there was an immediate burst of cyclooxygenase activity, indicating the presence of latent activity. A second addition of hydrogen peroxide after oxygen consumption slowed the second time had no effect (Fig. 11), indicating that no latent activity remained. The overall extent of oxygen consumption in the two bursts of activity was proportional to the amount of synthase added, indicating that the number of catalytic turnovers per synthase molecule before self-inactivation was independent of the fraction of the cyclooxygenase initiated in the first burst.

It is thus apparent that with EPA as substrate the rate of hydroperoxide generation is barely sufficient to sustain cyclooxygenase initiation in the face of the endogenous peroxidase activity. The preferential self-inactivation of the cyclooxygenase during catalysis also figures prominently, as it means that a relatively constant peroxidase capacity for hydroperoxide removal acts against a progressively lower cyclooxygenase capacity for hydroperoxide formation. The net result is that as the reaction proceeds the hydroperoxide concentration

eventually declines to a level unable to support efficient initiation of the remaining latent cyclooxygenase. These concepts also provide an explanation for earlier observations that EPA was not an effective cyclooxygenase substrate in the presence of phenol (34, 37). Those reactions were conducted at pH 8.5, where the cyclooxygenase activity is about one-third of that at pH 7.2, whereas the peroxidase activity is little affected (38). The higher pH thus leads to a pronounced shift in the ratio of peroxidase capacity to cyclooxygenase capacity, with the expected result that the endogenous peroxidase is able to keep the hydroperoxide from accumulating enough to support cyclooxygenase initiation and catalysis. However, without added cosubstrate, the endogenous peroxidase activity is vitiated, and enough hydroperoxide can accumulate for effective cyclooxygenase catalysis.

The detailed analysis of reaction kinetics made possible by the computer simulation thus provides important insights into the interaction between the two catalytic activities of the synthase and into the way that a quantitative difference between arachidonate and EPA in the oxygenation rate constant can lead to the observed qualitatively different kinetic phenomena.

#### Alternative Mechanisms

An earlier version of the mechanism shown in Fig. 1 postulated initiation of the cyclooxygenase from  $E^{IV}$  rather than from  $E^V$  (35). In this arrangement, a reducing cosubstrate could act to increase the rate of cyclooxygenase initiation by increasing the concentration of  $E^{IV}$ . This action would also decrease the concentration of  $E^V$  and thereby decrease the rate of self-inactivation via  $k_{DD}$ . It was anticipated (4) that these actions could account for the coordinate increases in the velocity and extent of the cyclooxygenase reaction observed with added cosubstrate (21). However, extensive simulations with this earlier mechanistic scheme proved unable to predict accurately the cosubstrate-dependent increase in cyclooxygenase reaction extent (not shown). Also, the earlier model predicted that the bulk of the enzyme would have heme in the ferric state during cyclooxygenase catalysis. It has been found instead that the synthase heme is mostly in the ferryl state during reaction with arachidonate (39). To avoid these difficulties, the mechanism was modified to have initiation of the cyclooxygenase from  $E^V$ , which would be likely to result in cyclooxygenase intermediates with ferryl heme (Fig. 1).

Another alternative mechanism has been proposed very recently by Hsuanyu and Dunford (40). In this mechanism,  $E^V$  itself abstracts the hydrogen atom from arachidonate forming fatty acid radical and  $E^{IV}$ . The fatty acid radical attacks oxygen to produce PGG<sub>2</sub>. Interaction of  $E^{IV}$  with reducing cosubstrate regenerates resting synthase to complete the cycle. Because  $E^V$  must be regenerated by reaction with hydroperoxide after each round of cyclooxygenase catalysis, this mechanism predicts that the peroxidase cycle is an integral part of the cyclooxygenase cycle. This prediction is difficult to reconcile with the observed differential inhibition of the two activities by GSH peroxidase (41). The mechanism also predicts that reduction of hydroperoxide should have a 1:1 stoichiometry with production of PGG<sub>2</sub> and that no net accumulation of PGG<sub>2</sub> should occur. However, significant levels of PGG<sub>2</sub> have been found to accumulate during cyclooxygenase activity in the presence of cosubstrate (13, 42). Thus, the overall mechanism proposed by Hsuanyu and Dunford (40) is not likely to account for a major part of cyclooxygenase catalysis.

A variant of the mechanism proposed by Hsuanyu and Dunford (40), with  $E^V$  itself as the cyclooxygenase oxidant

but with  $E^{IV}$  converted back to  $E^V$  by donation of a hydrogen atom to the PGG<sub>2</sub> radical, is another possibility. Such a mechanism would predict that many moles of PGG<sub>2</sub> are synthesized per mol of PGG<sub>2</sub> used to initiate the cyclooxygenase, consistent with the observation that accumulation of PGG<sub>2</sub> can occur (13, 42). However, such a mechanism would seem to be prone to strong inhibition by peroxidase cosubstrates because the redox centers of the principal cyclooxygenase intermediates are similar to those in the peroxidase intermediates. This would be difficult to reconcile with the observed stimulation of the cyclooxygenase by phenol.  $E^V$  has not been detected, even transiently, during reaction of the synthase with arachidonate (18, 20) although this could reflect a faster rate for its reaction with arachidonate than for its generation from  $E^{III}$  by PGG<sub>2</sub>.

Dietz *et al.* (20) first proposed that a tyrosyl radical was the initial intermediate in the cyclooxygenase reaction cycle. It has become clear that several structurally and temporally distinct tyrosyl radicals can be observed during peroxidase and/or cyclooxygenase reaction (19, 22, 43–46). The exact role (if any) each of these radicals play in synthase catalysis and self-inactivation remains controversial. Although the mechanistic model used (Fig. 1) is consistent with having a tyrosyl radical as  $E_C$ , the present simulations do not offer direct evidence as to the structure of the active cyclooxygenase intermediate. However, the quantitative framework developed here can be easily adapted to set kinetic boundaries for individual cyclooxygenase intermediates and thus help in evaluating the roles of putative intermediates in catalysis.

The studies reported here represent, to the best of our knowledge, the first comprehensive test of the ability of a mechanism similar to that proposed by Dietz *et al.* (20) to account for cyclooxygenase kinetic behavior under a wide variety of conditions. Much of this behavior was poorly understood. The unified kinetic model for the synthase generated satisfactory simulations of these cyclooxygenase reactions, and thus it provides a practical framework for interpretation of the influences of various agents and conditions on the synthesis of prostaglandins. The reaction simulations complement experimental observations by permitting a more detailed description of the probable changes in individual reaction intermediates. As illustrated by the self-suppression encountered with EPA as substrate, this detailed information can reveal unexpected and significant aspects of the ways in which the two activities of this important enzyme interact. This approach to analysis of complex cyclooxygenase kinetics should be quite useful to investigations of the similarities and differences between the two isoforms (9, 10) of this important enzyme.

#### REFERENCES

1. van der Ouderaa, F. J., Buytenhek, M., Nugteren, D. H., and van Dorp, D. A. (1977) *Biochim. Biophys. Acta* **487**, 315–331
2. Hemler, M. E., Cook, H. W., and Lands, W. E. M. (1979) *Arch. Biochem. Biophys.* **193**, 340–345
3. Smith, W. L., and Lands, W. E. M. (1972) *Biochemistry* **11**, 3276–3285
4. Kulmacz, R. J. (1986) *Arch. Biochem. Biophys.* **249**, 273–285
5. Lands, W., Lee, R., and Smith, W. (1971) *Ann. N. Y. Acad. Sci.* **180**, 107–122
6. Hemler, M. E., and Lands, W. E. M. (1980) *J. Biol. Chem.* **255**, 6253–6261
7. Smith, W. L., Eling, T. E., Kulmacz, R. J., Marnett, L. J., and Tsai, A.-L. (1992) *Biochemistry* **31**, 3–7
8. Marshall, P. J., Kulmacz, R. J., and Lands, W. E. M. (1987) *J. Biol. Chem.* **262**, 3510–3517
9. Xie, W., Chipman, J. G., Robertson, D. L., Erikson, R. L., and Simmons, D. L. (1991) *Proc. Natl. Acad. Sci. U. S. A.* **88**, 2692–2696
10. Kujubu, D. A., Fletcher, B. S., Varnum, B. C., Lim, R. W., and Herschman, H. R. (1991) *J. Biol. Chem.* **266**, 12866–12872
11. Graff, G. (1982) *Methods Enzymol.* **86**, 376–385
12. Kulmacz, R. J., and Lands, W. E. M. (1987) in *Prostaglandins and Related Substances: A Practical Approach* (Benedetto, C., McDonald-Gibson, R. G., Nigam, S., and Slater, T. F. eds) pp. 209–227, IRL Press, Washington, D. C.
13. Kulmacz, R. J. (1987) *Prostaglandins* **34**, 225–240

14. Lawrence, R. A., Sunde, R. A., Schwartz, G. L., and Hoekstra, W. G. (1974) *Exp. Eye Res.* **18**, 563-569
15. MacDonald, I. D., and Dunford, H. B. (1989) *J. Inorg. Biochem.* **37**, 35-44
16. Gunzler, W. A., Vergin, H., Muller, I., and Flohe, L. (1972) *Hoppe-Seyler's Z. Physiol. Chem.* **353**, 1001-1004
17. Chance, B. (1952) *Arch. Biochem. Biophys.* **41**, 416-424
18. Lambeir, A.-M., Markey, C. M., Dunford, H. B., and Marnett, L. J. (1985) *J. Biol. Chem.* **260**, 14894-14896
19. Kulmacz, R. J., Tsai, A.-L., and Palmer, G. (1987) *J. Biol. Chem.* **262**, 10524-10531
20. Dietz, R., Nastainczyk, W., and Ruf, H. H. (1988) *Eur. J. Biochem.* **171**, 321-328
21. Kulmacz, R. J., and Lands, W. E. M. (1985) *Prostaglandins* **29**, 175-190
22. Karthein, R., Dietz, R., Nastainczyk, W., and Ruf, H. H. (1988) *Eur. J. Biochem.* **171**, 313-320
23. Potter, D. W., and Hinson, J. A. (1987) *J. Biol. Chem.* **262**, 974-980
24. Moreno, S. N. J., Stolze, K., Janzen, E. G., and Mason, R. P. (1988) *Arch. Biochem. Biophys.* **265**, 267-271
25. Hsuanyu, Y., and Dunford, H. B. (1992) *Arch. Biochem. Biophys.* **292**, 213-220
26. Hsuanyu, Y., and Dunford, H. B. (1990) *Biochem. Cell Biol.* **68**, 965-972
27. Markey, C. M., Alward, A., Weller, P. E., and Marnett, L. J. (1987) *J. Biol. Chem.* **262**, 6266-6279
28. Marshall, P. J., and Kulmacz, R. J. (1988) *Arch. Biochem. Biophys.* **266**, 162-170
29. Pendleton, R. B. (1990) *Hydroperoxide Stimulation of Prostaglandin Endoperoxide Synthase*. Ph.D. thesis, University of Illinois at Urbana-Champaign
30. Hemler, M. E., Crawford, C. G., and Lands, W. E. M. (1978) *Biochemistry* **17**, 1772-1779
31. Marshall, P. J., Warso, M. A., and Lands, W. E. M. (1985) *Anal. Biochem.* **145**, 192-199
32. Kulmacz, R. J., Miller, J. F., Jr., Pendleton, R. B., and Lands, W. E. M. (1990) *Methods Enzymol.* **186**, 431-438
33. Ohki, S., Ogino, N., Yamamoto, S., and Hayaishi, O. (1979) *J. Biol. Chem.* **254**, 829-836
34. Culp, B. R., Titus, B. G., and Lands, W. E. M. (1979) *Prostaglandins Med.* **3**, 269-278
35. Pendleton, R. B., and Lands, W. E. M. (1991) in *Eicosanoids and Other Bioactive Lipids in Cancer and Radiation Injury* (Honn, K. V., Marnett, L. J., Nigam, S., and Walden, T., Jr., eds) pp. 209-212, Kluwer Academic Publishers, Norwell, MA
36. Marshall, P. J., Kulmacz, R. J., and Lands, W. E. M. (1984) in *Oxygen Radicals in Chemistry and Biology* (Bors, W., Saran, M., and Tait, D., eds) pp. 299-304, Walter de Gruyter & Co., Berlin
37. Lands, W. E. M., LeTellier, P. R., Rome, L. H., and Vanderhoek, J. Y. (1973) *Adv. Biosci.* **9**, 15-28
38. Kulmacz, R. J., and Lands, W. E. M. (1983) *Adv. Prostaglandin Thromboxane Leukotriene Res.* **11**, 93-97
39. MacDonald, I. D., and Dunford, H. B. (1989) *Biochem. Cell Biol.* **67**, 301-305
40. Hsuanyu, Y., and Dunford, H. B. (1992) *J. Biol. Chem.* **267**, 17649-17657
41. Kulmacz, R. J., and Lands, W. E. M. (1983) *Prostaglandins* **25**, 531-540
42. Eling, T. E., Glasgow, W. C., Curtis, J. F., Hubbard, W. C., and Handler, J. A. (1991) *J. Biol. Chem.* **266**, 12348-12355
43. Kulmacz, R. J., Ren, Y., Tsai, A.-L., and Palmer, G. (1990) *Biochemistry* **29**, 8760-8771
44. Lassmann, G., Odenwaller, R., Curtis, J. F., DeGray, J. A., Mason, R. P., Marnett, L. J., and Eling, T. E. (1991) *J. Biol. Chem.* **266**, 20045-20055
45. Tsai, A.-L., Palmer, G., and Kulmacz, R. J. (1992) *J. Biol. Chem.* **267**, 17753-17759
46. DeGray, J. A., Lassmann, G., Curtis, J. F., Kennedy, T. A., Marnett, L. J., Eling, T. E., and Mason, R. P. (1992) *J. Biol. Chem.* **267**, 23583-23588